The Pennsylvania State University

The Graduate School

College of Medicine

THE EFFECTS OF SCHWEINFURTHINS AND OTHER POTENTIAL CHEMOTHERAPIES ON DIFFUSE INTRINSIC PONTINE GLIOMA CELLS

A Thesis in

Anatomy

by

Daniel Daugherty

Submitted in Partial Fulfillment

of the Requirements

for the Degree of

Master of Science

May 2019

The thesis of Daniel Daugherty was reviewed and approved* by the following:

Jeffrey Neighbors

Assistant Professor of Pharmacology/Medicine

Thesis Advisor

Raymond Hohl

Director, Pennsylvania State Cancer Institute

Patricia McLaughlin

Professor, Department of Neural & Behavioral Sciences

Anatomy Program Director

*Signatures are on file in the Graduate School.

Abstract

Diffuse intrinsic pontine glioma is a brainstem tumor representing one of the deadliest pediatric cancers with a median overall survival of 8-14 months. Currently, the two-year survival rate is <10% and has remained that for over thirty years. No therapy provides a survival benefit; however, radiation is standard of care, providing temporary symptom relief. Over 250 clinical trials have failed; therefore, many drugs have been tested against multiple cell lines. Cyclin-dependent kinase inhibitors dinaciclib and SNS-032, as well as AKT inhibitor perifosine have all shown potent effects. Similarly, the University of Rochester has synthesized a compound specifically for diffuse intrinsic pontine glioma and it has shown effects in a mouse model. Lastly, schweinfurthins were found to have potent effects against the National Cancer Institute 60-cell line screen, including glioblastoma multiforme. They have been shown to indirectly inhibit AKT, decrease cholesterol synthesis, and increase cholesterol export. This study evaluated schweinfurthins and other potential chemotherapies in a cell culture model via human diffuse intrinsic pontine glioma cell line SF8628. TTI-3066, a schweinfurthin analog, increased p-AKT and Taz, while AKT, ABCA1, and PARP protein levels all decreased. TTI-3066 was also tested for synergy with radiation as well as the other chemotherapies. The cell line tested, SF8628, is very sensitive to TTI-3066 as an IC50 of 36 nM was reported. Although TTI-3066 does not appear to synergize with radiation, it does appear to synergize with SNS-032 at higher concentrations. Perifosine and dinaciclib in combination with TTI-3066 both display synergy. Lastly, the University of Rochester compound appears to synergize with radiation. Schweinfurthins have antiproliferative effects in diffuse intrinsic pontine glioma cell line SF8628, however other cell lines should be assessed and these mechanisms should be further explored. These results are promising for the future treatment of diffuse intrinsic pontine glioma.

Table of Contents

List of Figures

Abbreviations

ACVR1: Activin A Receptor Type I

AKT: Protein Kinase B

AML: Acute Myeloid Leukemia

ANOVA: Analysis of Variance

ATP: Adenosine Triphosphate

BBB: Blood Brain Barrier

BCA: Bicinchoninic Acid Assay

bFGF: Basic Fibroblast Growth Factor

CDK: Cyclin Dependent Kinase

CI: Combination Indices

CLL: Chronic Lymphocytic Leukemia

CNS: Central Nervous System

CV: Crystal Violet

DIPG: Diffuse Intrinsic Pontine Glioma

DMEM: Dulbecco's Modified Eagle Medium

EGF: Epidermal Growth Factor

ER: Endoplasmic Reticulum

GBM: Glioblastoma Multiforme

IC50: Inhibitory Concentration 50%

MM: Multiple Myeloma

mTOR: Mammalian Target of Rapamycin

MTT: 3-(4,5-Dimethylthiazol-2-Yl)-2,5-Diphenyltetrazolium Bromide

NCI: National Cancer Institute

p-AKT: Phosphorylated Protein Kinase B

PARP: Poly (ADP-Ribose) Polymerase

PDGF: Platelet Derived Growth Factor

PI3K: Phosphoinositide 3-Kinase

PVDF: Polyvinylindene Flouride

RIPA: Radioimmunoprecipitation Assay Buffer

SEM: Standard Error of the Mean

SDS: Sodium Dodecyl Sulfate

TTI: Terpenoid Therapeutics Incorporated

TP53: Tumor Protein 53

UR: University of Rochester

Acknowledgements

This study would not have been possible if not for the committee responsible for mentoring and revising the protocol, this committee includes Dr. Jeffrey Neighbors, Dr. Patricia McLaughlin, and Dr. Raymond Hohl. Special thanks should be given to the entire Hohl lab, some of whom taught me everything I know about cell culture. Lastly, Dr. Neighbors has been a wonderful mentor and is a very encouraging and thoughtful leader of students.

Chapter 1: Background of Diffuse Intrinsic Pontine Glioma, Schweinfurthins, and other potential chemotherapies

1.1 DIPG

Diffuse intrinsic pontine glioma (DIPG) is a pediatric brainstem tumor that infiltrates the ventral pons, accounts for 75-80% of all pediatric tumors, and 10-15% of all pediatric central nervous system tumors (Warren et al., 2012; Lapin et al., 2017). It is estimated that 100-150 new cases arise each year (Long et al., 2017). Although DIPG can occur in adults, the peak incidence is in children ages 5-10 and affects males and females equally (1:1). DIPG represents one of the deadliest cancers in children with a median survival of 8-14 months from the time of diagnosis (Vanan and Eisenstat, 2015) and the two-year survival rate is <10% (Long et al., 2017).

1.1.1 Clinical Incidence, Symptoms, and Genotyping

Patients are usually diagnosed within 2-3 months of clinical symptoms. The classic triad of symptoms includes cerebellar signs (ataxia), long-tract signs (clonus), and cranial nerve palsies (double vision). Tumors are not resected and generally not biopsied due to the anatomical location on the pons and it being critical for life sustaining functions (Warren et al., 2012). Currently, no therapy provides any survival benefit; however, radiation therapy is the standard treatment, providing temporary symptom relief (Long et al., 2017). Chemotherapeutic crossing of the blood brain barrier (BBB) is a major obstacle for treatment of brainstem tumors (Vanan and Eisenstat, 2015). Over 250 clinical trials have failed as the survival has remained static over the last 25-30 years (Madrid et al., 2015). This has led to the recent analysis of DIPG through genomic sequencing of autopsy and biopsy samples. Nearly 80% of DIPG harbor a histone H3 lysine 27 to methionine mutation. This mutation is the most prevalent followed by platelet derived growth factor (PDGF, 32%), ACVR1 (20-32%), and tumor protein 53 (TP53,

22-40%) among many others that show lower but significant mutation rates (Lapin et al., 2017). Genetic analysis could elicit multiple potential targets and combined therapies that were not considered before.

1.1.2 Potential Targets for DIPG

Due to the characteristic of cancer cells to be fast growing, a common target for cancer therapies is cell proliferation. Cholesterol biosynthesis, in particular, has been shown to be essential for cell proliferation (Singh et al, 2013). The brain is the most cholesterol-rich organ in the body, accounting for roughly 20% of the total body cholesterol (Dietschy, 2009). However, cholesterol itself cannot cross the blood brain barrier (BBB) and must be synthesized de novo by astrocytes (Dietschy and Turley, 2001). The PI3K/AKT pathway, via PDGF, controls the metabolic flux of glucose and glutamine to the de novo synthesis of cholesterol (Guo et al., 2011; Lapin et al., 2017). Similarly, addictive glycolysis is a main feature of cancer cells and is also upregulated by the PI3K/AKT pathway. This up-regulation leads to fatty acid synthesis (Guo et al., 2014). Indirectly targeting this AKT pathway that regulates cholesterol flux and metabolism in the brain via schweinfurthins could synergize with a direct AKT inhibitor due to their different mechanisms. Furthermore, DIPG growth creates a hypoxic environment that causes an entire metabolic reprogramming of tumor cells. Instead of relying on vasculature for nutrients; the tumor cells rely even more heavily on glycolysis and de novo lipogenesis (Nguyen et al., 2017). Lastly, depletion of cellular cholesterol leads to the death of glioblastoma multiforme (GBM) cells, another highly aggressive brain tumor that also relies heavily on cholesterol for survival (Villa et al., 2016). Therefore, targeting a pathway such as this could elicit a potential synergistic target against DIPG cells. As cholesterol is needed for biological membranes and cell

proliferation, targeting cholesterol and the cell cycle in tandem could lead to a synergistic effect. For this reason, CDK inhibitors and schweinfurthins provide a potential route of synergy.

1.2 Schweinfurthins

The National Cancer Institute (NCI) Developmental Therapeutics Program developed a 60-cell line program, including lung, CNS, renal, colon, leukemia, ovarian, breast and prostate cancers, that is used to test a variety of drugs against different tumor types (Close et al., 2018; Shoemaker, 2006). Since its creation in the 1990s over 100,000 compounds have been tested using various cell lines to obtain a profile of drug interactions, mechanisms, and profiles. Drugs with closely related mechanisms have similar actions and therefore mechanisms can be predicted on unknown drugs (Close et al., 2018). Schweinfurthins were first isolated from the plant *Macaranga schweinfurthii* in the late 1990s by the NCI Program. They were found to have very potent and differential activity in the 60-cell line screen. Interestingly, schweinfurthins demonstrated potent growth inhibition against central nervous system cancer cell lines, specifically the glioblastoma multiforme (GBM) cell lines, such as SF-295 and SF-539 (Kuder et al., 2009). Development of the naturally occurring schweinfurthins for cancer therapy has been hindered by limited availability. Therefore, synthesis of schweinfurthins was undertaken and several analogs were created that maintained the cytotoxic profiles of the natural product schweinfurthin B. These included 3-deoxyschweinfurthin B (3dSB), the fluorescent 3-deoxyschweinfurthin B p-nitro bis-stilbene (3dSB-PNBS), 5′-methylschweinfurthin G (methyl-G), among others (Sheehy et al., 2015). Schweinfurthin G was shown to decrease AKT phosphorylation prior to apoptosis (Bao et al, 2015). These schweinfurthins have been shown to induce ER stress and suppress lipid-raft mediated PI3K activation and mTOR complex activation leading to mTOR/AKT inhibition (Koubek et al., 2018). Similarly, a decrease in total cholesterol

was shown after schweinfurthin treatment that appears to be due to impaired cholesterol biosynthesis and increased cholesterol export but the mechanism is still unclear (Koubek et al., 2018). Targeting cholesterol pathways may be key to stopping proliferation of tumor cells.

1.3 DIPG and Other Potential Chemotherapies

DIPG growth creates a hypoxic environment that leads to an entire metabolic reprogramming of these cells. This is driven by mutations in TP53, AKT/PI3K and mTOR pathway, and MYC, all of which have been identified in DIPG (Nguyen et al., 2017; Lapin et al., 2017). Many drugs, including but not limited to CDK and AKT inhibitors, have shown promise against 14 different DIPG cells lines (Grasso et al., 2015). Specifically, Dinaciclib and SNS-032 are two potent CDK inhibitors that were shown to be potent against DIPG. Dinaciclib selectively inhibits CDK 1, 2, 5, and 9. It has been shown to be effective against multiple myeloma, relapsed and refractory chronic lymphocytic leukemia, and in ovarian carcinoma xenograft models (Flynn et al., 2015; Kumar et al., 2015). SNS-032 inhibits CDK 2 and 9, and has effects on CDK 7. It has been tested against acute myeloid leukemia, chronic lymphocytic leukemia, multiple myeloma, and in human ovarian carcinoma xenograft models (Walsby et al., 2011; Chen et al., 2009). Perifosine is an AKT inhibitor that has also shown potent effects against DIPG. Perifosine has been shown to have *in vitro* antitumor effects against melanoma, nervous, lung, prostate, colon, and breast cancers. It has also been shown to induce apoptosis in human leukemia cells and to be beneficial with radiation (Richardson et al., 2012). Similarly, UR-8, an analog of GSK-J4, was synthesized by the University of Rochester. It has shown *in* vivo effects in a mouse model of DIPG. Lastly, due to radiation being the standard of care for DIPG, perifosine could be used in combination therapies with radiation in children with DIPG.

Chapter 2: Specific Aims and Hypothesis

The long-term goal of this research is to provide a preliminary study on the effects of schweinfurthins on DIPG cells. Schweinfurthins have shown potent activity against other CNS tumors but have never been tested against DIPG. Similarly, this study aims to explore potential synergistic combinations with drugs shown to have potent effects against multiple DIPG cell lines. Due to the link between AKT and cholesterol synthesis in the brain, targeting these two pathways simultaneously with drugs that utilize different mechanisms could work to synergize in DIPG. Similarly, rapidly proliferating cancer cells need to bypass cell cycle checkpoints and their need for cholesterol for membranes, targeting cholesterol and cell cycle regulators could provide another synergistic route in DIPG. The methods are designed to test the effects of schweinfurthins on DIPG cell proliferation via cholesterol and the PI3K/AKT pathway in adherent monolayer human DIPG cell line SF8628. *I hypothesize that TTI-3066 treatment will impair metabolic activity and cell proliferation of DIPG cell line SF8628 via MTT and crystal violet respectively. Similarly, TTI-3066 will display synergy with dinaciclib, SNS-032, perifosine, and radiation.*

Chapter 3: Methodology

3.1 Cell Culture and Drugs

SF8628 was acquired through Millipore Sigma and is a pediatric diffuse intrinsic pontine glioma (DIPG) cell line harboring the histone H3.3 lysine 27-to-methionine (K27M) mutation. SF8628 was cultured in DMEM as an adherent monolayer and were incubated at 37°C. Dinaciclib is a potent inhibitor of cyclin dependent kinases 1, 2, 5, and 9 and was purchased from Adooq Biosciences. SNS-032 is an ATP-competitive inhibitor of cyclin dependent kinases 9, 2, and 7 and was purchased from Selleck Chemicals. Perifosine is an AKT inhibitor and was purchased from Tocris. A compound, UR-8, was given as a generous gift from the University of Rochester synthesized specifically for DIPG and has shown *in vivo* effects. Schweinfurthins came from Terpenoid Therapeutics Incorporated (TTI) under material transfer agreement with the PSU PSCI.

3.2 MTT Assay

MTT assays tested the metabolic activity of SF8628 after TTI-3114, TTI-4242, or TTI-3066 treatment. Following the initial MTT, TTI-3066 was the only schweinfurthin used. Cells were seeded at 5,000 cells/well in a 96-well plate to yield 80% confluency after overnight incubation. The following day, each drug in phenol red-free DMEM was added. TTI-3066, TTI-4242, TTI-3114, and SNS-032 were added in log dilutions from 100 pM to 10 μM, and UR-8 was added at 10, 25, 50, 75, 100, and 150 μM. Dinaciclib was used in log dilutions from 1 nM to 100 μM. Lastly, Perifosine was used in concentrations of 1, 10, 50, 75, 100, and 250 μM. DMSO in cell media will be used as a negative control. Each MTT will be 48 hours treatment. After 44 hours of incubation, MTT salt was added to each well. Plates were returned to culturing

conditions for 4 hours. Reduction of the MTT salt was halted by the addition of stop solution (80% isopropanol, 10% hydrochloric acid, 10% Triton X). Plates were then incubated at 37 °C overnight. The assay was quantified by measuring the optical density of wells at 570 nm and 690 nm (reference wavelength) using a SpectraMax i3x (Molecular Devices, Sunnyvale, CA). Reduced values were calculated by subtracting values of 570 and 690 nm for each well.

3.2.1 Radiation

Radiation was used in conjunction with MTT as both a control and to test synergy as this is a common therapy for DIPG. Cells were seeded at 5,000 cells/well in a 96-well plate to yield 80% confluency after overnight incubation. The following day, TTI-3066 in phenol red-free DMEM was added in log dilutions from 100 pM to 10 μM, and UR-8 was added at 10, 25, 50, 75, 100, and 150 μM. Cells treated with TTI-3066 were radiated at timepoints of 0, 6, 12, 18, and 24 hours after drug administration. For UR-8, cells were radiated after 24 hours of treatment. Cells were placed in rubber bins while transporting to radiation facilities to keep the cells warm. After 44 hours of drug incubation, MTT salt was added to each well. Plates were returned to culturing conditions for 4 hours. Reduction of the MTT salt was halted by the addition of stop solution (80% isopropanol, 10% hydrochloric acid, 10% Triton X). Plates were then incubated at 37 °C overnight. Cells were radiated using an X-Rad 320 iX (Precision X-Ray Inc., North Branford, CT). The assay was quantified by measuring the optical density of wells at 570 nm and 690 nm (reference wavelength) using a SpectraMax i3x (Molecular Devices, Sunnyvale, CA). Reduced values were calculated by subtracting values of 570 and 690 nm for each well.

3.3 Crystal Violet

Crystal violet staining was used to test effect of Perifosine, Dinaciclib, SNS-032, TTI-3114, TTI-4242, or TTI-3066 treatment as a secondary test of cell viability. Cells were grown to 80% confluency then a Crystal Violet Cell Cytotoxicity Assay Kit was used. Cells were seeded at 5,000 cells/well in a 96-well plate to yield 80% confluency after overnight incubation. The following day, each drug in phenol red-free DMEM was added. TTI-3066, TTI-4242, TTI-3114, and SNS-032 was added in log dilutions from 100 pM to 10 μM. Dinaciclib was used in concentrations of 1 nM to 100 μM. Lastly, Perifosine was used in concentrations of 1, 10, 50, 75, 100, and 250 μM. DMSO in cell media was used as a negative control. After 48 hours of incubation, cells were stained with 0.5% crystal violet solution in 30% ethanol for 20 minutes (Sigma-Aldrich Corp., St. Louis, MO, USA), rinsed with di$H_2$0, and dried. When the plates dried, a methanol extraction solution was applied and the plate placed on a shaker for 20 minutes (Feoktistova et al., 2016). The degree of stain was quantified by measuring the optical density of wells at 570 nM.

3.4 Western Blotting

Western blotting was used to test for apoptosis by detection of cleaved caspase 9, and PARP. Similarly, levels of p-AKT and panAKT were also tested as it has been stated before that schweinfurthins indirectly inhibit p-AKT levels. ABCA1 will be tested to verify previous results showing the cholesterol exporter protein levels increasing after schweinfurthin treatment. Lastly, Taz will be looked at as Taz has been shown to be partially controlled by the mevalonate pathway (Sorrentino et al., 2014). Cells were seeded in 10 cm plates at a cell density of $1x10^6$ cells/plate and grown to 60-70% confluency. MTT assay was used to determine a concentration of TTI-3066 that impairs cell proliferation without causing significant cell death. The next day, cells were treated with DMSO in DMEM (vehicle) or TTI-3066. After 24 or 48 hours, cells were

lysed with RIPA buffer with protease inhibitor cocktail (10 mM Tris-Cl pH 8.0, 1 mM EDTA, 0.1% SDS, 140 mM NaCl). Lysate was rotated at 4C for 1 hour then centrifuged at 13,000 g for 10 minutes. Protein content of supernatant was quantified by BCA assay and equal amounts of protein resolved by SDS and transferred to PVDF membrane. The membranes were probed overnight for cleaved Caspase-9 (Cell Signaling Technology), ABCA1 (Cell Signaling Technology), PARP 1/2 (Santa Cruz Biotechnology), Taz (Cell Signaling Technology), AKT-Thr308 (Cell Signaling Technology), pan AKT (Cell Signaling Technology), Vinculin (Cell Signaling Technology, loading control), and GAPDH (Cell Signaling Technology, loading control). The membrane was then probed with secondary antibodies from ScanLater™ Western Blot Assay Kit (Molecular Devices). Caspase-9 and Caspase-8 were probed for goat anti-mouse while all other membranes were probed with goat anti-rabbit. Signal was detected using the ScanLater™ Western Blot Detection cartridge for the SpectraMax® and quantified using ImageStudio Lite. panAKT, p-AKT-Thr308, and PARP 1/2 signals were normalized to GAPDH. All others were normalized to Vinculin. All western blots are the result of 1 biological replicate.

3.5 Isobologram Analysis and Synergy

Synergy was tested via isobologram analysis of MTT data using CompuSyn software (Combosyn, Inc.) (Tallarida, 2011). An MTT assay was used in which TTI-3006 was plated in log dilutions from 100 pM to 10 μM. Along with TTI-3066, either perifosine, SNS-032, or dinaciclib was plated in concentrations of 10, 25, 50, and 75 μM; 10 nM, 50 nM, 100 nM, and 1 μM; and 10 nM, 50 nM, 100 nM, and 100 μM respectively for 48 hours. Synergy between TTI-3066 and radiation was also explored by increasing concentrations of TTI-3066 with 300 rads. Drug interactions were analyzed graphically (Chou, 2006). Combination index (CI) values were

extrapolated where CI=1 portrays additive effects; CI<1 suggests synergy; and a CI >1 displays antagonism between the two drugs (Holstein and Hohl, 2001).

3.6 Statistical Analysis

All data are reported as mean +/- SEM and is in triplicate unless otherwise stated. Paired t-tests were used to test for statistical significance. Differences with P-value < .05 were considered statistically significant. Statistical analysis was performed using GraphPad Prism software. Combination index data was calculated using CompuSyn.

Chapter 4: Results

4.1 MTT and Crystal Violet

Schweinfurthins have been tested in numerous cancer cell lines and animal models but have yet to be tested in any DIPG cell line (Koubek et al., 2018). Therefore, initial cell viability experiments were initiated to investigate effects on the metabolic activity of SF8628 DIPG cell line through MTT assays. All three drugs were used in log doses from 100 pM to 10 μM and show a dose dependent reduction in metabolic activity. TTI-3066 showed an IC50 of 36 nM, TTI-3114 an IC50 of 60 nM, and TTI-4242 an IC50 of 2 μM. Overall, DIPG was more sensitive to TTI-3066 than TTI-3114 and TTI-4242 respectively (Figure 4.1). Similarly, as an indirect quantification of cell death and proliferation, CV assays were undertaken. A concentration-dependent reduction of cell viability as measured by optical density was shown for TTI-3066, TTI-3114, and TTI-4242 (Figure 4.1). TTI-3066 showed an IC50 of 182 nM, TTI-3114 an IC50 of 486.7 nM, and TTI-4242 an IC50 of 41.8 nM from crystal violet assays.

DIPG has no effective treatment and therefore the screening of any drugs thought to be effective has been undertaken (Grasso et al., 2015). If an effective treatment is to be found for DIPG, synergy must be an explored path. Among those shown effective in 14 different DIPG cell lines were CDK inhibitors, SNS-032 and dinaciclib, as well as AKT inhibitor, perifosine (Grasso et al., 2015). SNS-032 was used in log concentrations from 100 pM to 10 μM; dinaciclib from 1 nM to 100 μM; and perifosine in concentrations of 1, 10, 50, 75, 100, and 250 μM. All three inhibitors showed a concentration-dependent decrease in metabolic activity (Figure 2). CDK inhibitor SNS-032 displays an IC50 of 37 nM (Figure 2A). AKT inhibitor perifosine displays an IC50 of 93 μM (Figure 2B). CDK Inhibitor dinaciclib displays an IC50 of 23 nM (Figure 4.2C). Lastly, UR-8 was synthesized specifically for DIPG at the University of Rochester

and displays dose dependent decreases in metabolic activity (Figure 4.2D). UR-8 displayed an IC50 of 35 μM (Figure 4.2D).

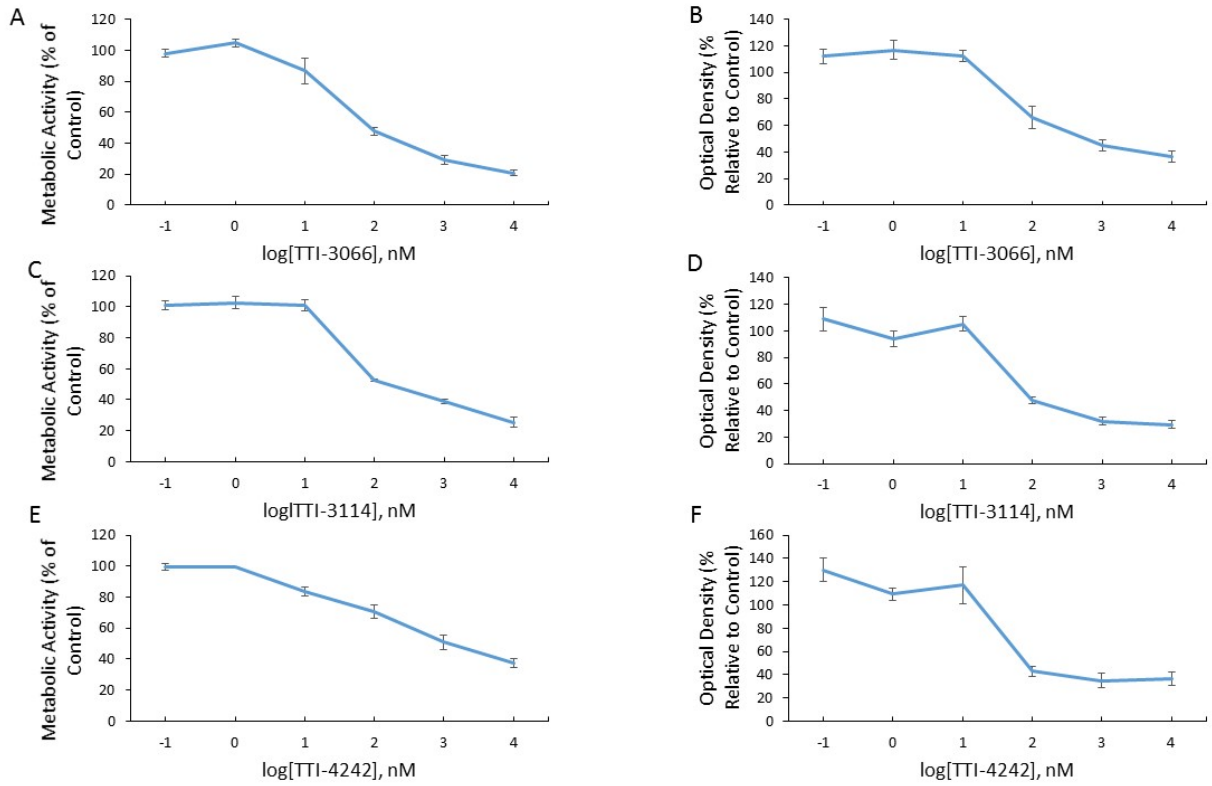

Figure 4.1. Left: Treatment with three schweinfurthin analogs, TTI-3066, TTI-3114, and TTI-4242 concentration-dependently decreased metabolic activity of SF8628 DIPG cells. Metabolic activity was determined using an MTT and is expressed relative to DMSO-treated control. **Right**: Crystal violet assay shows a concentration-dependent reduction of cell viability. CV was read at 570 nM. **A**: MTT displaying log[TTI-3066]. **B**: CV displaying log[TTI-3066]. **C**: MTT displaying log[TTI-3114]. **D**: CV displaying log[TTI-3114]. **E**: MTT displaying log[TTI-4242]. **F**: CV displaying log[TTI-4242]. **A-F** are all done in SF8628 with log concentrations of 100 pM to 10 μM. All data are expressed as mean +/- SEM with three independent experiments done in triplicate.

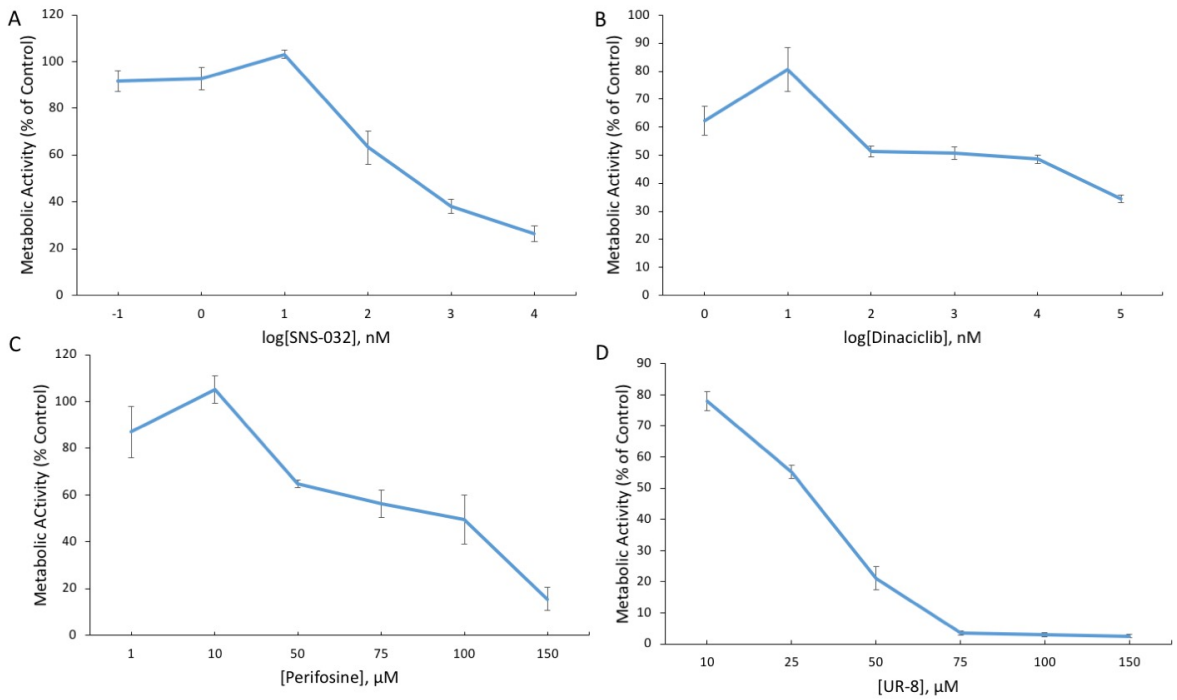

Figure 4.2. Initial dose response MTT for potential synergistic additions to schweinfurthins concentration-dependently decreased metabolic activity of SF8628 DIPG cells. Metabolic activity was determined using an MTT and is expressed relative to DMSO-treated control. **A:** Initial MTT of CDK inhibitor SNS-032 using log dilutions from 100 pM to 10 µM. **B:** Initial MTT of CDK inhibitor dinaciclib using log dilutions from 1 nM to 100 µM. **C:** Initial MTT of AKT inhibitor perifosine using concentrations of 1, 10, 50, 75, 100, and 250 µM. **D:** Initial MTT of UR-8 using concentrations of 10, 25, 50, 75, 100, and 150 µM. All data are expressed as mean +/- SEM with three independent experiments done in triplicate.

4.2 Western Blot

This study proposed inhibition of cell viability would be through a decrease in p-AKT levels and intracellular cholesterol. In order to test this, western blotting of total AKT and p-

AKT was completed. Although schweinfurthins have been shown to decrease intracellular cholesterol in other cancers, ABCA1 was tested to investigate these levels of a cholesterol exporter in DIPG cells. Also, apoptosis was tested via PARP 1 cleavage. Lastly, Taz was looked at because the mevalonate pathway has been shown to partially control it.

Protein levels of p-AKT were shown to increase across all treatments with a more substantial effect in the 48-hour treatments (Figure 4.3B). Similarly, protein levels of AKT decrease across all treatments (Figure 4.3C). There is an overall increase in protein levels of Taz across both treatment groups, however there is not a clear trend to this increase (Figure 4.4B). Total PARP levels display an overall decrease after TTI-3066 treatment, outside of one treatment group. No cleaved PARP band was present (Figure 4.5B). Similarly, cholesterol exporter ABCA1 displayed an overall decrease in protein levels, outside of one group (Figure 4.6B).

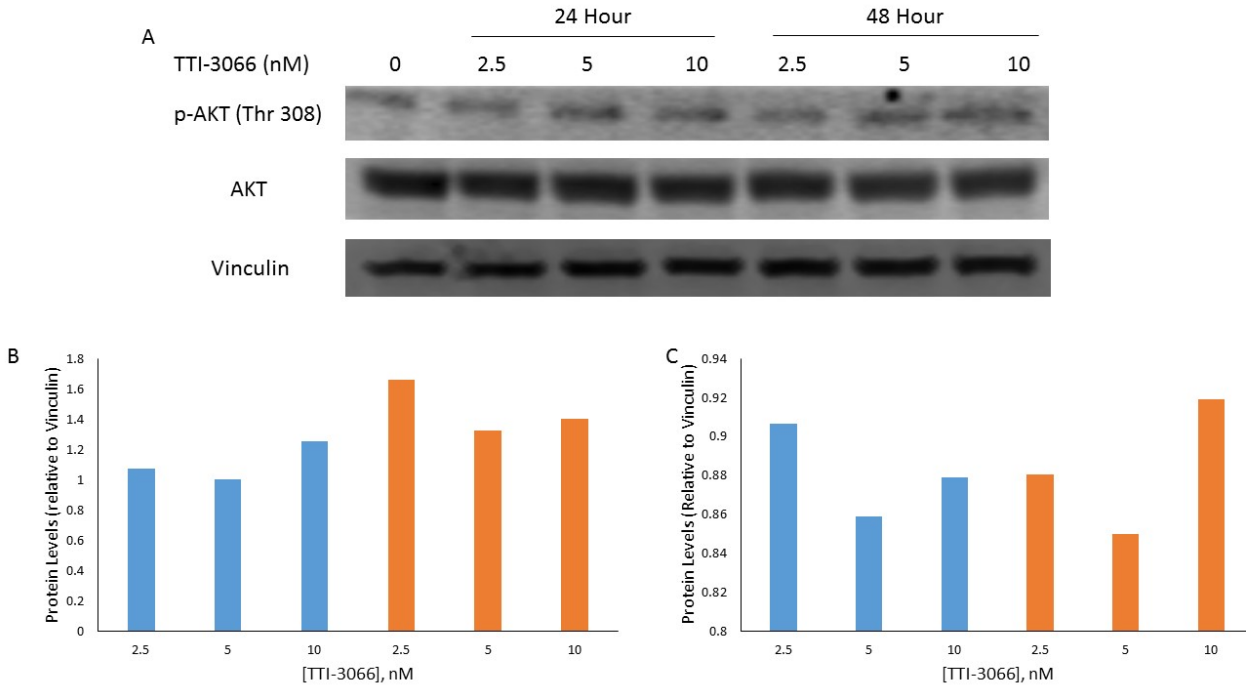

Figure 4.3. Western blot analysis of p-AKT (Thr 308) and panAKT. **A:** SF8628 cells treated with TTI-3066 at concentrations of 2.5, 5, and 10 nM at 24 (blue bars) and 48-hour (orange bars) timepoints. **B:** p-AKT (Thr 308) intensity relative to loading control (Vinculin) and vehicle. **C:** panAKT intensity relative to loading control (Vinculin) and vehicle.

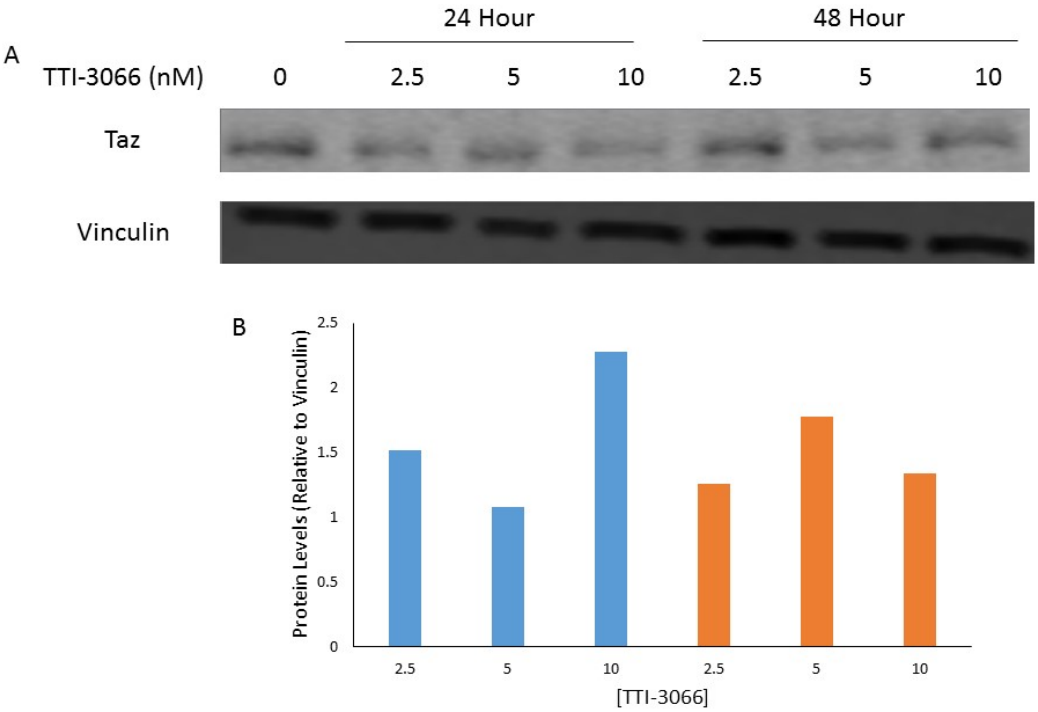

Figure 4.4. Western blot analysis of Taz. **A:** SF8628 cells treated with TTI-3066 at concentrations of 2.5, 5, and 10 nM at 24 (blue bars) and 48-hour (orange bars) timepoints. **B:** Taz intensity relative to loading control (Vinculin) and vehicle.

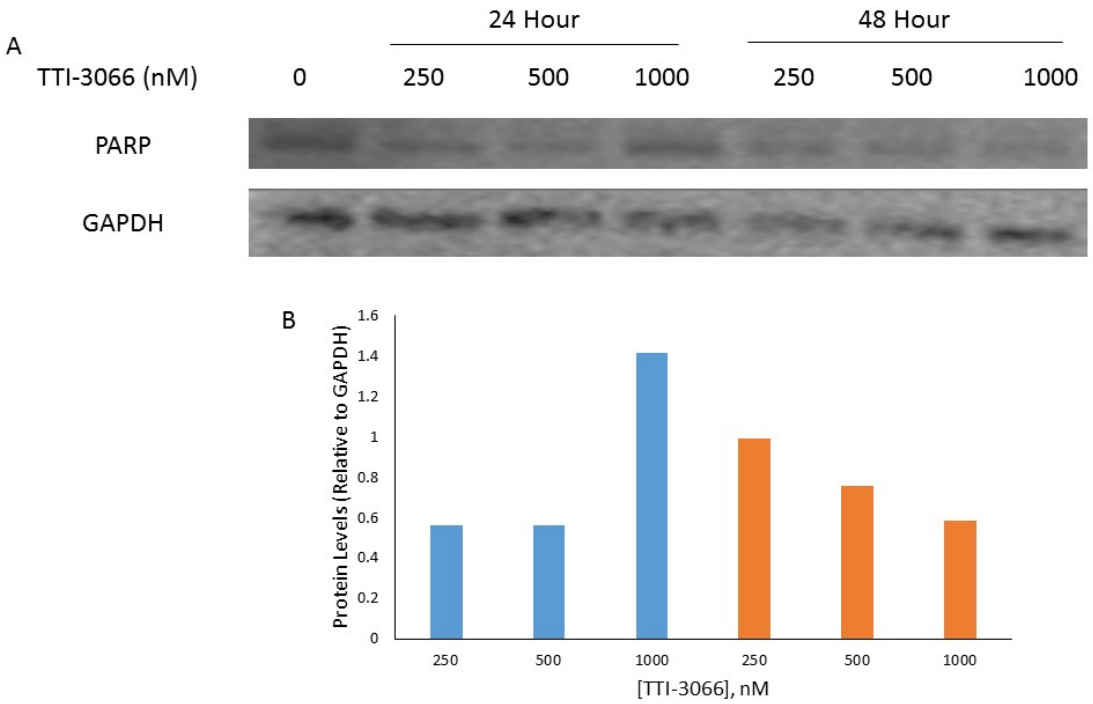

Figure 4.5. Western blot analysis of PARP. **A:** SF8628 cells treated with TTI-3066 at concentrations of 250, 500, and 1000 nM at 24 (blue bars) and 48-hour (orange bars) timepoints. **B:** PARP intensity relative to loading control (GAPDH) and vehicle.

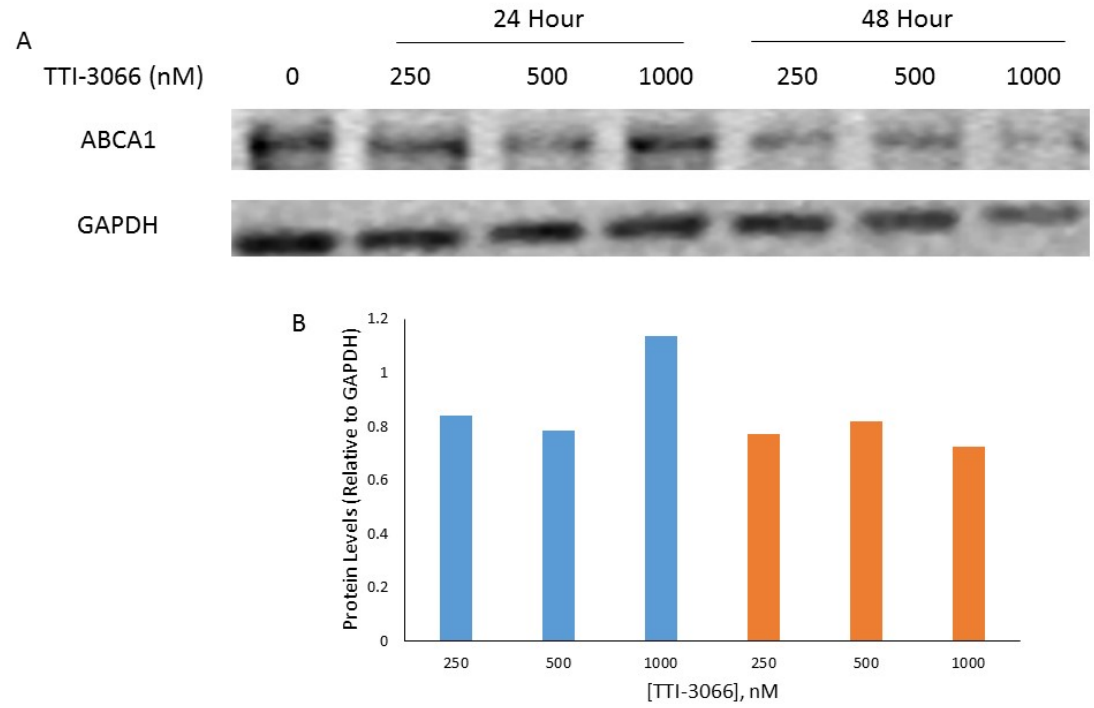

Figure 4.6. Western blot analysis of ABCA1. **A:** SF8628 cells treated with TTI-3066 at concentrations of 250, 500, and 1000 nM at 24 (blue bars) and 48-hour (orange bars) timepoints. **B:** ABCA1 intensity relative to loading control (GAPDH) and vehicle.

4.3 Synergy Analysis

Common cancer therapies include a "drug cocktail" to enhance the effects of drugs and limit the desensitization of the specific cancer to targeted therapies, especially when targeting the PI3K/AKT pathway (Matthew and Rutka, 2018). Therefore, this study aimed to test schweinfurthins with other therapies that are proven to be effective. Initially, 300 rads of radiation was looked at in combination with increasing log concentrations of TTI-3066 from 10 pM to 1 μM across multiple timepoints because standard of care for DIPG patients is radiation therapy (Long et al., 2017). It appears that the combination of TTI-3066 and radiation do not display synergy; the effects seem to be additive, at least with the 6-hour timepoint (Figure 4.7A).

Secondly, when compared to their control, UR-8 appeared to be synergistic with radiation as there is a great reduction in metabolic activity (Figure 4.7B). Data for UR-8 with radiation are in duplicate, not triplicate. Radiation in combination with 10 and 25 μM of UR-8 showed statistical significance (P=0.048). Similarly, 50 μM UR-8 with radiation was very significant (P=0.005) (Figure 4.7B). After 50 μM, all SF8628 cells appear to be dead.

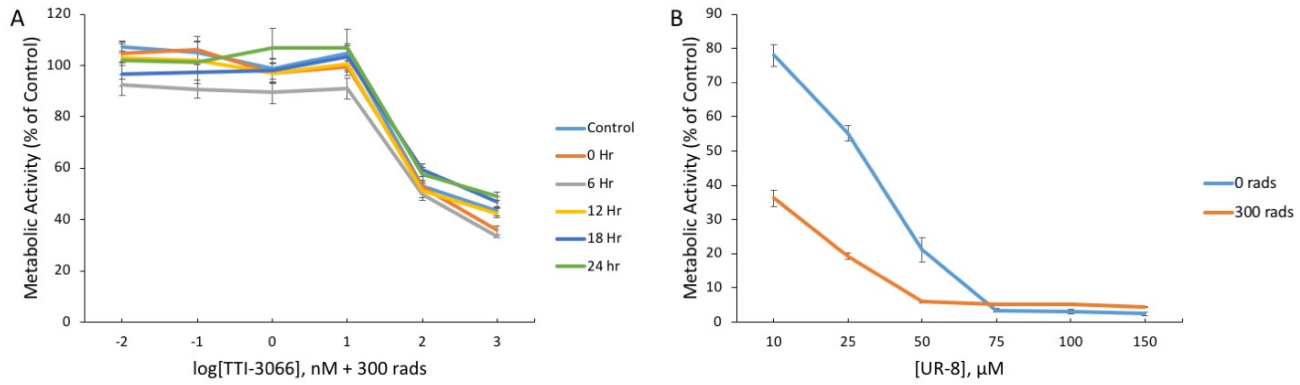

Figure 4.7. Radiation study on both TTI-3066 (A) and UR-8 (B). MTT was performed and radiation was administered using an X-Rad 320 iX (Precision X-Ray Inc., North Branford, CT). **A:** MTT of log[TTI-3066] from 10 pM to 1 μM in combination with 300 rads of radiation in timepoints of 0, 6, 12, 18, and 24 hours after drug administration. **B:** MTT of UR-8 using concentrations of 10, 25, 50, 75, 100, and 150 μM in combination with 300 rads of radiation. All data are shown as mean +/- SEM and are independent experiments done in triplicate unless otherwise stated.

Schweinfurthins have shown potent effects on the metabolic activity of DIPG cells (Figure 4.1). Testing schweinfurthins with other chemotherapies that have been shown to be effective against DIPG in cell culture could provide a synergistic route to impairing the

proliferation of these deadly cancer cells. TTI-3066 is used in concentrations from 100 pM to 10 μM in all experiments for synergy testing. When TTI-3066 is combined with AKT inhibitor perifosine, the effects are potent (Figure 4.8A). There appears to be a synergistic combination between the two drugs. 10 μM perifosine when combined with 100 pM, 1, and 10 nM TTI-3066 displays very significant results (P= 0.005). 25 μM perifosine displayed statistical significance at 10 nM TTI-3066 (P=0.02). 50 μM perifosine also displayed significance at 100 pM, 1, and 10 nM individually (P=0.03, 0.006, <.0001). Lastly, when 75 μM perifosine is combined with TTI-3066 there is statistical significance at every concentration (P=0.04). When CDK inhibitor SNS-032 is used in combination with TTI-3066 the effects are minimal, outside of one concentration that a potent effect has been shown (Figure 4.8B). 50 nM SNS-032 when combined with TTI-3066 at 1 nM concentration is very significant (P=0.0096). Similarly, at 10 μM SNS-032 in combination with TTI-3066 there is statistical significance at every concentration (P=0.041). When CDK inhibitor Dinaciclib is used in combination with TTI-3066 the effects are rather potent (Figure 4.8C). 10 nM dinaciclib in combination with 100 pM TTI-3066 is statistically significant (P=0.002). 50 nM dinaciclib in combination with 100pM-10nM TTI-3066 is also significant (P=0.025). 100 nM dinaciclib in combination with 100 pM-100nM TTI-3066 there is statistical significance (P=0.0065). 100 μM dinaciclib in combination with TTI-3066 shows statistical significance at every concentration (P=0.0024). When 25 μM perifosine is combined with TTI-3066 there is strong antagonism, however when 75 μM perifosine is combined with TTI-3066 synergy is displayed (Figure 4.9B-C). As stated previously, the combination of TTI-3066 and dinaciclib displayed very potent effects (Figure 4.10). After analysis of MTT data, the combination index provides a representation of synergy at three of the four concentrations of dinaciclib used (Figure 4.10B-D). At 50 nM, 100 nM, and 100 μM dinaciclib in combination

with log concentrations of TTI-3066 from 100 pM to 10 µM there is strong synergy outside of two data points where the curves overlap at high concentrations (Figure 4.10 B-D).

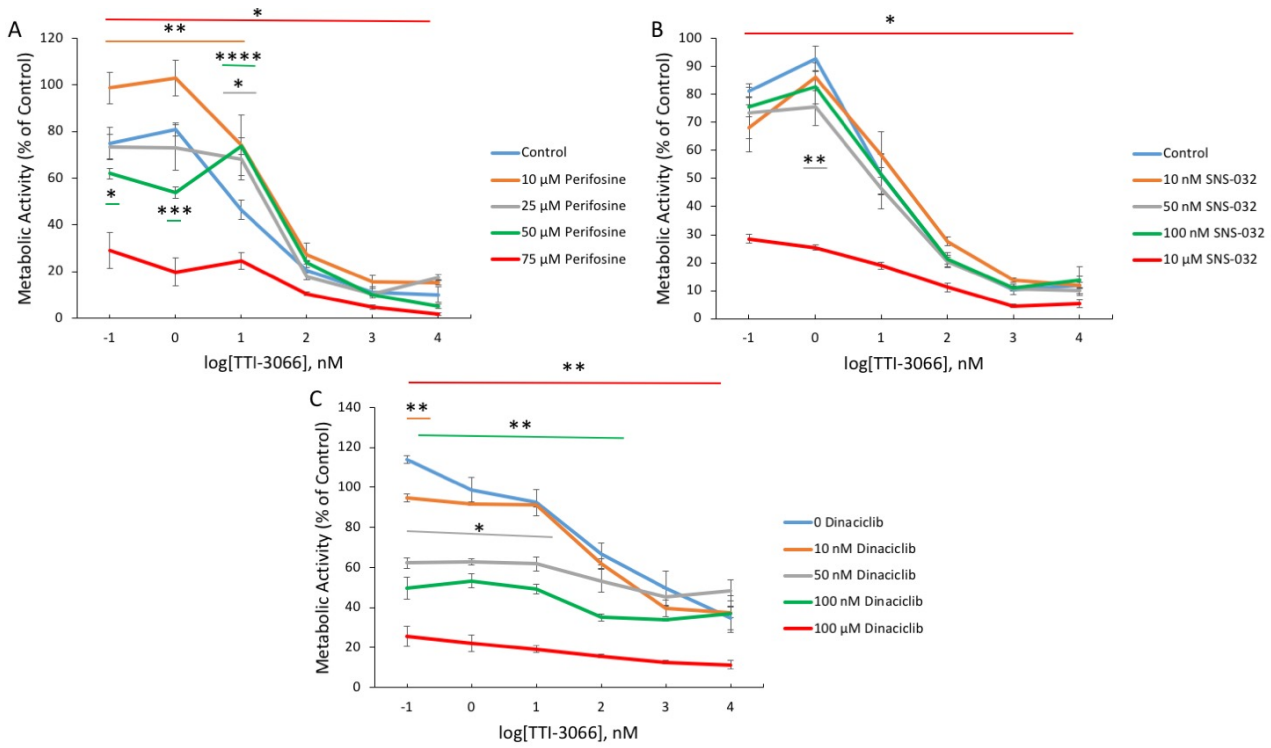

Figure 4.8. Synergy study combining potential chemotherapies in addition to increasing log concentrations of TTI-3066. **A:** MTT of log[TTI-3066] from 100 pM to 10 µM in combination with 0, 10, 25, 50, or 75 µM perifosine. **B:** MTT of log[TTI-3066] from 100 pM to 10 µM in combination with 0, 10, 50, 100 nM, or 10 µM SNS-032. **C:** MTT of log[TTI-3066] from 100 pM to 10 µM in combination with 0, 10, 50, 100 nM, or 100 µM dinaciclib. Results are shown as mean +/- SEM and all data are the result of one independent experiment in duplicate.

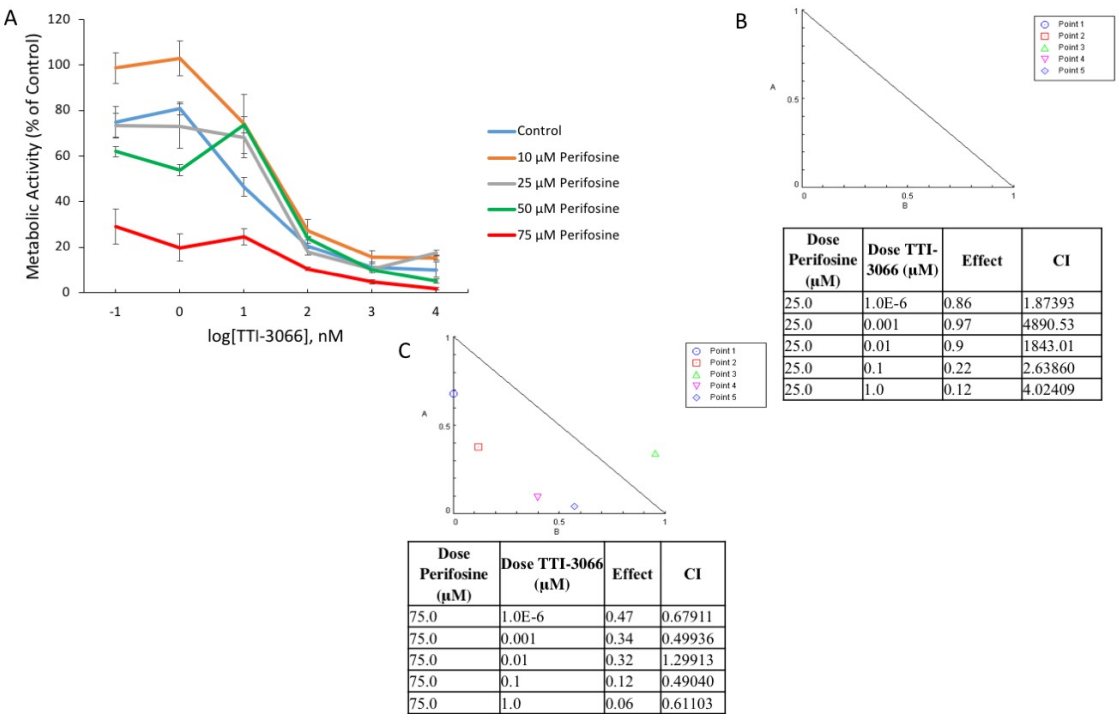

Dose Perifosine (µM)	Dose TTI-3066 (µM)	Effect	CI
25.0	1.0E-6	0.86	1.87393
25.0	0.001	0.97	4890.53
25.0	0.01	0.9	1843.01
25.0	0.1	0.22	2.63860
25.0	1.0	0.12	4.02409

Dose Perifosine (µM)	Dose TTI-3066 (µM)	Effect	CI
75.0	1.0E-6	0.47	0.67911
75.0	0.001	0.34	0.49936
75.0	0.01	0.32	1.29913
75.0	0.1	0.12	0.49040
75.0	1.0	0.06	0.61103

Figure 4.9. Synergistic combination of perifosine and TTI-3066. **A:** MTT of perifosine and TTI-3066. **B:** Graph and table with combination index data showing antagonism of 25 µM perifosine with TTI-3066. **C:** Graph and table with combination index data showing synergy of 75 µM perifosine with TTI-3066.

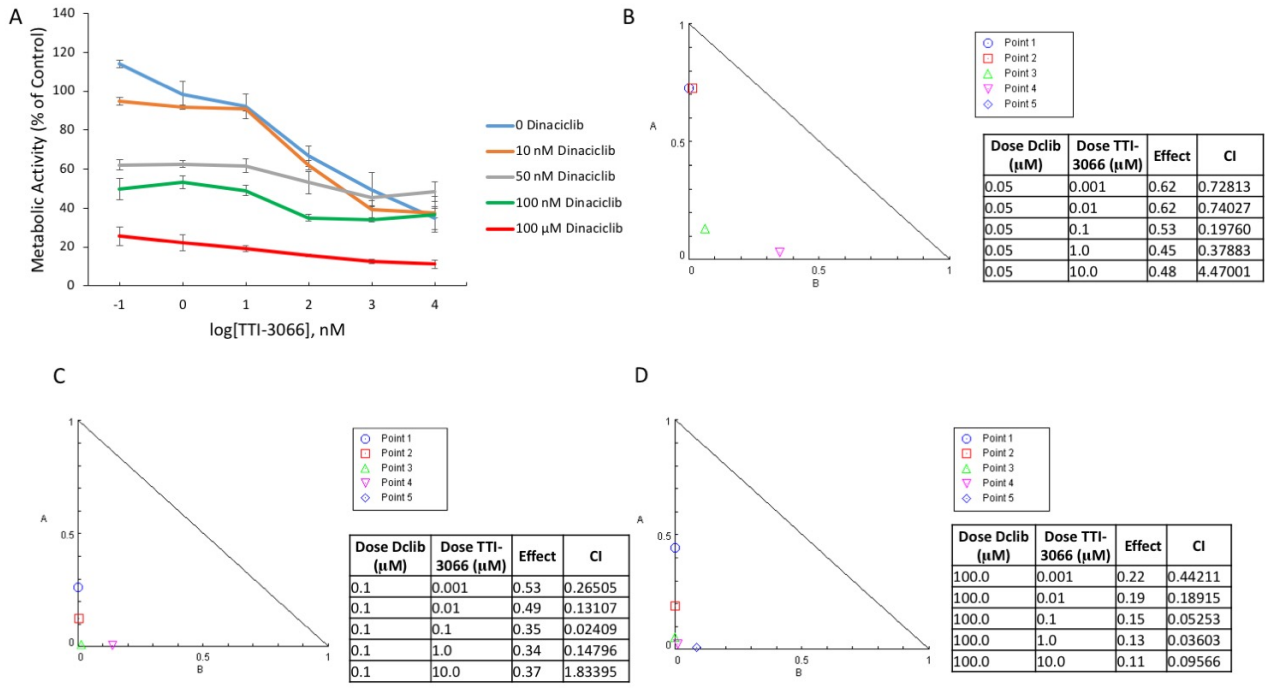

Dose Dclib (µM)	Dose TTI-3066 (µM)	Effect	CI
0.05	0.001	0.62	0.72813
0.05	0.01	0.62	0.74027
0.05	0.1	0.53	0.19760
0.05	1.0	0.45	0.37883
0.05	10.0	0.48	4.47001

Dose Dclib (µM)	Dose TTI-3066 (µM)	Effect	CI
0.1	0.001	0.53	0.26505
0.1	0.01	0.49	0.13107
0.1	0.1	0.35	0.02409
0.1	1.0	0.34	0.14796
0.1	10.0	0.37	1.83395

Dose Dclib (µM)	Dose TTI-3066 (µM)	Effect	CI
100.0	0.001	0.22	0.44211
100.0	0.01	0.19	0.18915
100.0	0.1	0.15	0.05253
100.0	1.0	0.13	0.03603
100.0	10.0	0.11	0.09566

Figure 4.10. Synergistic combination of dinaciclib and TTI-3066. **A:** MTT of dinaciclib and TTI-3066. **B:** Graph and table with combination index data showing synergy of 50 nM dinaciclib with TTI-3066. **C:** Graph and table with combination index data showing synergy of 100 nM dinaciclib with TTI-3066. **D:** Graph and table with combination index data showing synergy of 100 µM dinaciclib with TTI-3066.

Chapter 5: Discussion

The potent effects of schweinfurthins against the NCI-60 cell cancer screen, and in particular, against the NCI CNS cell line panel led this study to test TTI-3066 against DIPG. Schweinfurthins have been shown to greatly reduce intracellular cholesterol levels in GBM cell lines, which largely make up the NCI CNS panel. These decreased cholesterol levels are via decreased cholesterol synthesis and increased cholesterol efflux (Kuder et al., 2015). Cholesterol biosynthesis, in particular, has been shown to be essential for cell proliferation (Singh et al, 2013). Similarly, the brain is the most cholesterol rich organ in the body and therefore should be a target for antiproliferative therapies for DIPG (Dietschy, 2009).

DIPG is a pediatric brainstem tumor that is not only invariably fatal but is a cancer whose therapeutic approach remains elusive (Long et al., 2017, Madrid et al., 2015, Vanan and Eisenstat, 2015). This study proposed that the inhibition of AKT alongside increased cholesterol export would lead to an impairment of proliferation of DIPG cells. Although results are achieved through different assays, based upon the characterization of the antiproliferative activity of schweinfurthins in 60 human cancer cell lines, the low nanomolar IC50 for TTI-3066, TTI-4242, and TTI-3114 indicate a sensitivity of DIPG cell line SF8628 to schweinfurthin analogs (Figure 1) (Bao et al., 2015). Establishing this baseline in a DIPG cell line is promising due to the lack of therapy available to patients. This study is the first to test schweinfurthin analogs against DIPG cells and the results display promise for the therapeutic approach to DIPG.

In order to test whether or not TTI-3066 treatment impaired AKT/p-AKT, western blot analysis was completed. This study showed that TTI-3066 leads to an increase in p-AKT while decreasing total AKT levels (Figure 4.3B-C). An increase in p-AKT protein levels shows the PI3K/AKT pathway is still active and working. The decrease in total AKT could be due to the

increase in p-AKT. Although these data are the result of one biological replicate, it appears that TTI-3066 is not inhibiting p-AKT at this low concentration, however at a higher concentration of TTI-3066 this could be achieved as previously shown (Bao et al., 2015).

Schweinfurthins have been shown to have effects on the mevalonate pathway, and in turn, has shown to decrease Taz protein levels (Koubek et al., 2018). Taz is one transcriptional activator that is partially controlled by the mevalonate pathway and leads to differentiation and growth (Sorrentino et al., 2014). This study investigated the effects of TTI-3066 of Taz protein levels and found that there was an overall increase in Taz levels although there is not a trend in this increase (Figure 4.4B). An increase in Taz protein levels could lead to an increase in proliferation and differentiation of cells. Although this is contrary to what was shown before, this is the result of one biological replicate.

Schweinfurthins were also shown to induce PARP cleavage as an indication of apoptosis (Koubek et al., 2018). Although this study shows an overall decrease in PARP levels, the cleaved band was not present in the results (Figure 4.5B). This decrease could be due to an increase in the PARP being cleaved and therefore indicating apoptosis. However, without the cleaved band being present this is just speculation.

It was previously shown that cholesterol exporter ABCA1 expression decreases after schweinfurthin treatment. Similarly, a decrease in total cholesterol synthesis was also shown (Bao et al., 2015). It was shown in this study that protein levels of ABCA1 decrease after TTI-3066 treatment indicating less cholesterol export. This is contrary to previous published results and would indicate a different mechanism for TTI-3066's antiproliferative effects; however, these are the results of one biological replicate.

Due to the lack of therapy and the standard of care being radiation, the effects of radiation on drug combinations should be a focus of any study on DIPG. Although SF8628 was sensitive to schweinfurthins, the addition of 300 rads did not provide a synergistic combination, however, and possibly more importantly, it did not display antagonism (Figure 4.7A). On the contrary, the combination of UR-8 and radiation did appear to synergize (Figure 4.7B). The effects shown with UR-8 and radiation are promising and could yield a novel therapeutic target for DIPG patients.

The potent, low nanomolar IC50 of TTI-3066 against SF8628 provides a promising avenue for the treatment of DIPG. Although the PI3K/AKT/mTOR pathway presents a potential targeted therapy due to the upregulation of PDGFR in DIPG, inhibition of this pathway alone has shown inconclusive results in clinical trials investigating lung, prostate, colorectal, and bladder cancers (Wu et al., 2017; Lapin et al., 2017). For this reason, combination therapy with schweinfurthins may allow inhibition of the PI3K/AKT/mTOR pathway to be sufficient to impair DIPG. However, the results of this study do not show an inhibition of AKT as there is an increase in p-AKT protein levels at site Thr308. P-AKT at site Ser473 did not yield any results, however this should be tested to investigate whether TTI-3066 does in fact inhibit p-AKT. CDK inhibitors allow cells to be arrested in the cell cycle, directly inhibiting proliferation of cancer cells. Multiple CDK inhibitors have been shown efficacious in DIPG cells lines (Grasso et al., 2015). The first step to test this is to investigate the combination of AKT inhibitor and CDK inhibitors with schweinfurthins in DIPG cells. AKT inhibitor perifosine, as well as CDK inhibitor dinaciclib, appear to synergize with TTI-3066 (Figure 4.8A and C). However, the combination of dinaciclib and TTI-3066 appears to be killing the cells as there is no sigmoidal curve present at high concentrations (Figure 4.8C). Combination index data for perifosine show

extreme antagonism at 25 μM but synergy with 75 μM. Although not validated, the antagonism at lower concentrations of perifosine could be due to the increase in p-AKT seen via western blotting analysis of SF8628 treated with TTI-3066. This increase in p-AKT along with an inhibition of AKT would lead to antagonistic effects. Similarly, the synergy seen with perifosine is at such high concentrations the effects may be "off-target" of AKT leading to more widespread effects. The dual inhibition of AKT via perifosine along with a decrease in cholesterol via schweinfurthins could provide a novel targeted therapy for DIPG patients. Dinaciclib and perifosine previously showing potent effects against multiple DIPG cell lines and the data from this study showing potential synergy could be an effective approach in the long-term treatment of DIPG (Grasso et al., 2015). Perifosine has been shown to be safe and efficacious in clinical trials of sarcoma patients and dinaciclib in leukemia patients (Bailey et al., 2006; Flynn et al., 2015).

Schweinfurthins have been shown to be effective in one DIPG cell line, however there are other DIPG cell lines that were unable to be tested or unavailable to use. In order to confirm these results, schweinfurthins should be tested in multiple DIPG cell lines that include both adherent monolayer and neurosphere culture, as these culture methods have been shown to determine response to targeted therapies (Meel et al., 2017). Similarly, different proliferation assays should be undertaken to confirm the results shown in this study. Mechanistic studies should also be done to understand how schweinfurthins are affecting DIPG cells. Cholesterol added back to further test the theory that a decrease in intracellular cholesterol is the mechanism behind this inhibition. Due to the decrease in ABCA1 as shown in the results, increased cholesterol export may not be the mechanism that is working to impair proliferation and metabolic activity of SF8628 DIPG cells; however western blot data are from one biological

replicate and therefore these results should not be heavily relied on until replicated. Although only done in a cell line model, the results in this study could pave the way for TTI-3066 treatment in mouse models of DIPG. It has been reported that AKT inhibition alone is not enough to impair proliferation of DIPG in clinical trials (Flannery et al., 2018). However, this study showed a direct AKT inhibitor, perifosine, synergizing with TTI-3066. This combination could be enough to provide the antiproliferative effects needed to halt DIPG in animal models and in future clinical trials. One area of high value not seen in cell culture is the relationship between systems/pathways in the body and their influence on each other. For instance, the PI3K/AKT pathway in humans controlling the *de novo* synthesis of cholesterol in the brain is not seen in cell culture. Inhibition of this pathway would, in turn, limit cholesterol in the brain. These effects are not seen in cell culture and would elicit another route for the synergy of TTI-3066 and perifosine to yield antiproliferative effects in a clinical trial.

Lastly, the synergy shown with dinaciclib provides a very interesting look into CDK inhibition of DIPG in cell culture. This synergy is shown even with low concentrations that would be achievable in humans, providing a promising route of treatment for patients. As stated previously, dinaciclib is a CDK 1, 2, 5, and 9 inhibitor and displays synergy. However, SNS-032 is a CDK 2 and 9 inhibitor and did not show synergy. The differential effects shown between these two CDK inhibitors could be in the inhibition of CDK 1 and 5. Inhibiting these two is a possible explanation for the synergy seen with TTI-3066 and further experiments should be done to investigate if CDK 1 and 5 inhibitors synergize with schweinfurthins and whether these are shown to be more potent in DIPG than other CDK inhibitors like shown here. Although CDK 1 and 5 inhibitors are not currently being tested in DIPG, CDK 4 and 6 inhibitors abemaciclib, palbociclib, and ribociclib are shown to be efficacious in DIPG and abemaciclib has been shown

to cross the BBB (Mills et al., 2017; Asby, 2018). These results shown with CDK 1 and 5 inhibitors synergizing with TTI-3066 in DIPG cell line SF8628 could be a novel therapeutic target for DIPG that was previously unknown.

This study has some limitations, the first of which is validation of TTI-3066 effects in more than one cell line. There are many DIPG cell lines, however, not many are available to researchers. Similarly, the radiation study had many non-optimal variables in the protocol. Chief of which was the fact that the radiation building was roughly a mile from the lab. MTT plates were kept in rubber tubs to maintain warmth; however, no CO_2 was present. Radiation studies lasted about thirty minutes until plates were returned to their incubators. Another limitation was trouble with western blotting. The major problem with western blotting was lack of bands appearing on the membrane. Due to this limitation, only one biological replicate was established. Similarly, membranes were probed for Caspase 9, Caspase 8 and p-AKT at site Ser473 with no bands present. The last major limitation of this study was a lack of time. Having roughly only 8 months to gather data along with learning new protocols and figuring out how to radiate cells in a sterile cell culture environment limited the results produced.

Appendix

The following are figures that display results that did not meet standards or are excessive to the results reported above.

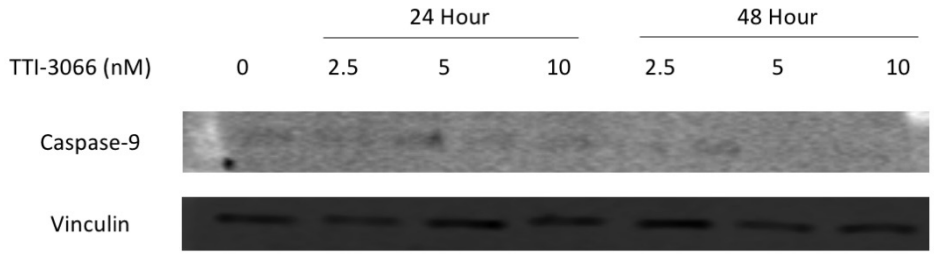

Caspase 9 Western blot with poor bands

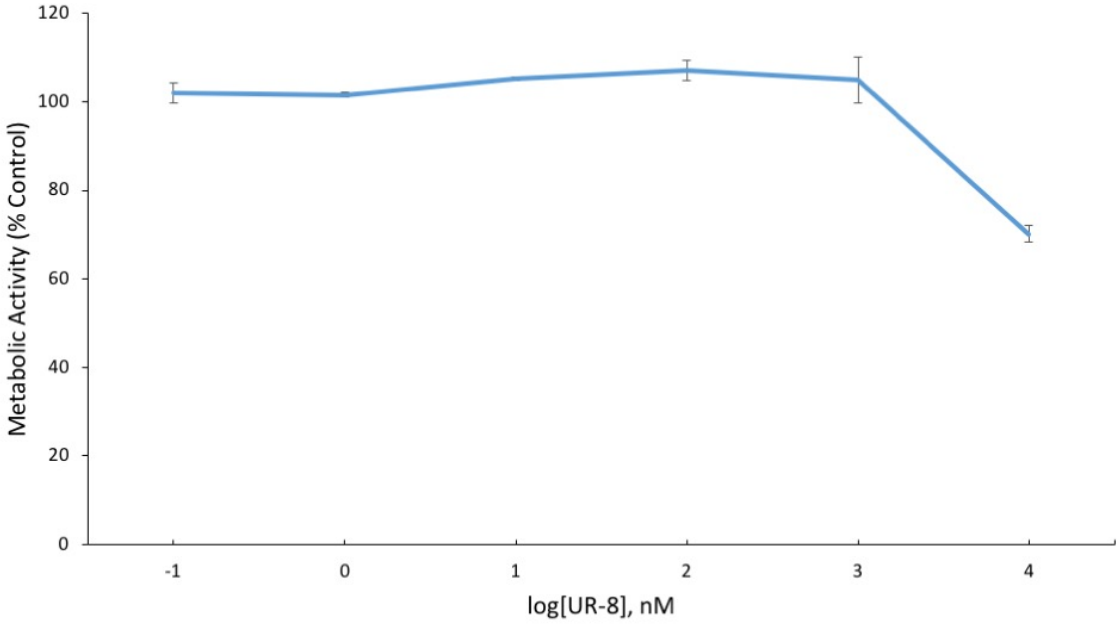

Initial MTT with UR-8 displaying minimal effects at a lower concentration than used in the results section

Bibliography

Asby, D., Bienemann, A., Wright, L., Singleton, W., Killick-Cole, C., Barua, N., Gill, S. "The combination of the CDK4/6 inhibitor Palbociclib with the rapalogue Temosirolimus inhibits DIPG cell proliferation via synergistic attenuation of cell cycle regulators." *Neuro-Oncology*, Volume 19, Issue supplement 4 (2017).

Bailey, H. H., M. R. Mahoney, D. S. Ettinger, W. J. Maples, P. M. Fracasso, A. M. Traynor, C. Erlichman, and S. H. Okuno. "Phase II Study of Daily Oral Perifosine in Patients with Advanced Soft Tissue Sarcoma." *Cancer* 107, no. 10 (2006): 2462-467. doi:10.1002/cncr.22308.

Bao, W. Zheng, N. H. Sugi, K. L. Agarwala, Q. Xu, Z. Wang, K. Tendyke, W. Lee, L. Parent, W. Li, H. Cheng, Y. Shen, N. Taylor, Z. Dezso, H. Du, Y. Kotake, N. Zhao, J. Wang, M. Postema, M. Woodall-Jappe, Y. Takase, T. Uenaka, D. G I Kingston, and K. Nomoto. "Small Molecule Schweinfurthins Selectively Inhibit Cancer Cell Proliferation and MTOR/AKT Signaling by Interfering with Trans-Golgi-network Trafficking." *Cancer Biology & Therapy* 16, no. 4 (2015): 589-601. doi:10.1080/15384047.2015.1019184.

Chen, Y., S. Germano, C. Clements, J. Samuel, G. Shelmani, S. Jayne, M. J. S. Dyer, and S. Macip. "Pro-survival Signal Inhibition by CDK Inhibitor Dinaciclib in Chronic Lymphocytic Leukaemia." *British Journal of Haematology* 175, no. 4 (2016): 641-51. doi:10.1111/bjh.14285.

Chen, R., W. G. Wierda, S. Chubb, R. E. Hawtin, J. A. Fox, M. J. Keating, V. Gandhi, and W. Plunkett. "Mechanism of Action of SNS-032, a Novel Cyclin-dependent Kinase Inhibitor, in

Chronic Lymphocytic Leukemia." *Blood* 113, no. 19 (2009): 4637-645. doi:10.1182/blood-2008-12-190256.

Chou, T. (2006). Theoretical Basis, Experimental Design, and Computerized Simulation of Synergism and Antagonism in Drug Combination Studies. *Pharmacological Reviews, 58*(3), 621-681. doi:10.1124/pr.58.3.10

Close, D. A., Wang, A. X., Kochanek, S. J., Shun, T., Eiseman, J. L., & Johnston, P. A. (2018). Implementation of the NCI-60 Human Tumor Cell Line Panel to Screen 2260 Cancer Drug Combinations to Generate 3 Million Data Points Used to Populate a Large Matrix of Anti-Neoplastic Agent Combinations (ALMANAC) Database. *SLAS DISCOVERY: Advancing Life Sciences R&D*. doi:10.1177/2472555218812429

Collins, K; Jacks, T; & Pavletich, NP. (1997). The cell cycle and cancer. *Proceedings of the National Academy of Sciences of the United States of America, 94*(7), 2776-2778. 10.1073/pnas.94.7.2776 Retrieved from https://www.jstor.org/stable/41721

Dietschy, J. M. (2009). Central nervous system: Cholesterol turnover, brain development and neurodegeneration. *Biological Chemistry, 390*(4), 287. 10.1515/BC.2009.035 Retrieved from http://www.ncbi.nlm.nih.gov/pubmed/19166320

Feoktistova, M., Geserick, P., & Leverkus, M. (2016). Crystal Violet Assay for Determining Viability of Cultured Cells. *Cold Spring Harbor Protocols, 2016*(4). doi:10.1101/pdb.prot087379

Flynn, J., J. Jones, A. J. Johnson, L. Andritsos, K. Maddocks, S. Jaglowski, J. Hessler, M. R. Grever, E. Im, H. Zhou, Y. Zhu, D. Zhang, K. Small, R. Bannerji, and J. C. Byrd.

"Dinaciclib Is a Novel Cyclin-dependent Kinase Inhibitor with Significant Clinical Activity in Relapsed and Refractory Chronic Lymphocytic Leukemia." *Leukemia* 29, no. 7 (2015): 1524-529. doi:10.1038/leu.2015.31.

Grasso, C. S., Y. Tang, N. Truffaux, N. E. Berlow, L. Liu, M. A. Debily, M. J. Quist, L. E. Davis, E. C. Huang, P. J. Woo, A. Ponnuswami, S. Chen, T. B. Johung, W. Sun, M. Kogiso, Y. Du, L. Qi, Y. Huang, M. Hütt-Cabezas, K. E. Warren, L. Le, P. S. Meltzer, H. Mao, M. Quezado, D. G. Van, J. Abraham, M. Fouladi, M. N. Svalina, N. Wang, C. Hawkins, J. Nazarian, M. M. Alonso, E. H. Raabe, E. Hulleman, P. T. Spellman, X. N. Li, C. Keller, R. Pal, J. Grill, and M. Monje. "Functionally Defined Therapeutic Targets in Diffuse Intrinsic Pontine Glioma." Current Neurology and Neuroscience Reports. June 2015. Accessed March 11, 2019. https://www.ncbi.nlm.nih.gov/pubmed/25939062.

Guo, D., F. Reinitz, M. Youssef, C. Hong, D. Nathanson, D. Akhavan, D. Kuga, A. N. Amzajerdi, H. Soto, S. Zhu, I. Babic, K. Tanaka, J. Dang, A. Iwanami, B. Gini, J. Dejesus, D. D. Lisiero, T. T. Huang, R. M. Prins, P. Y. Wen, H. I. Robins, M. D. Prados, L. M. Deangelis, I. K. Mellinghoff, M. P. Mehta, C. D. James, A. Chakravarti, T. F. Cloughesy, P. Tontonoz, and P. S. Mischel. "An LXR Agonist Promotes Glioblastoma Cell Death through Inhibition of an EGFR/AKT/SREBP-1/LDLR-Dependent Pathway." *Cancer Discovery* 1, no. 5 (2011): 442-56. doi:10.1158/2159-8290.cd-11-0102.

Guo, D; Bell, EH; Mischel, P; & Arnab Chakravarti. (2014). Targeting SREBP-1-driven lipid metabolism to treat cancer. *Current Pharmaceutical Design, 20*(15), 2619-2626. 10.2174/13816128113199990486 Retrieved from

http://www.eurekaselect.com/openurl/content.php?genre=article&issn=1381-6128&volume=20&issue=15&spage=2619

Holstein, S. A., & Hohl, R. J. (2001). Interaction of cytosine arabinoside and lovastatin in human leukemia cells. *Leukemia Research, 25*(8), 651-660. doi:10.1016/s0145-2126(00)00162-4

Koubek, E. J., Weissenrieder, J. S., Neighbors, J. D., & Hohl, R. J. (2018). Schweinfurthins: Lipid Modulators with Promising Anticancer Activity. *Lipids, 53*(8), 767-784. doi:10.1002/lipd.12088

Kuder, C. H., Sheehy, R. M., Neighbors, J. D., Wiemer, D. F., & Hohl, R. J. (2012). Functional evaluation of a fluorescent schweinfurthin: Mechanism of cytotoxicity and intracellular quantification. *Molecular Pharmacology, 82*(1), 9-16. 10.1124/mol.111.077107 Retrieved from http://www.ncbi.nlm.nih.gov/pubmed/22461663

Kuder, C. H., Neighbors, J. D., Hohl, R. J., & Wiemer, D. F. (2009). Synthesis and biological activity of a fluorescent schweinfurthin analogue. *Bioorganic & Medicinal Chemistry, 17*(13), 4718-4723. doi:10.1016/j.bmc.2009.04.071

Kuder, C. H., Weivoda, M. M., Zhang, Y., Zhu, J., Neighbors, J. D., Wiemer, D. F., & Hohl, R. J. (2015). 3-Deoxyschweinfurthin B Lowers Cholesterol Levels by Decreasing Synthesis and Increasing Export in Cultured Cancer Cell Lines. *Lipids, 50*(12), 1195-1207. doi:10.1007/s11745-015-4083-z

Kumar, S. K., B. Laplant, W. J. Chng, J. Zonder, N. Callander, R. Fonseca, B. Fruth, V. Roy, C. Erlichman, and A. K. Stewart. "Dinaciclib, a Novel CDK Inhibitor, Demonstrates

Encouraging Single-agent Activity in Patients with Relapsed Multiple Myeloma." *Blood* 125, no. 3 (2014): 443-48. doi:10.1182/blood-2014-05-573741.

Lamprecht, J., Wójcik, C., Jakóbisiak, M., Stoehr, M., Schrorter, D., & Paweletz, N. (1999). Lovastatin induces mitotic abnormalities in various cell lines. *Cell Biology International, 23*(1), 51-60. 10.1006/cbir.1998.0322 Retrieved from https://www.sciencedirect.com/science/article/pii/S1065699598903225

Lapin, D. H., Tsoli, M., & Ziegler, D. S. (2017). Genomic insights into diffuse intrinsic pontine glioma. *Frontiers in Oncology*.

Mathew, R. K., & Rutka, J. T. (2018). Diffuse Intrinsic Pontine Glioma: Clinical Features, Molecular Genetics, and Novel Targeted Therapeutics. *Journal of Korean Neurosurgical Society, 61*(3), 343-351. doi:10.3340/jkns.2018.0008

Meel, M., Sewing, A., Waranecki, P., Metselaar, D., Wedekind, L., Koster, J., Van Vuurden, D., Kaspers, G., and Hulleman, E. "Culture Methods of Diffuse Intrinsic Pontine Glioma Cells Determine Response to Targeted Therapies." *Experimental Cell Research* 360, no. 2 (2017): 397-403. doi:10.1016/j.yexcr.2017.09.032.

Mills, C. C., Kolb, E., & Sampson, V. B. (2017). Recent Advances of Cell-Cycle Inhibitor Therapies for Pediatric Cancer. *Cancer Research, 77*(23), 6489-6498. doi:10.1158/0008-5472.can-17-2066

Miwa, Y., Sasaguri, T., Kosaka, C., Taba, Y., Ishida, A., Abumiya, T., & Kubohara, Y. (2000). Differentiation-inducing factor-1, a morphogen of dictyostelium, induces G(1) arrest and

differentiation of vascular smooth muscle cells. *Circulation Research, 86*(1), 68. Retrieved from http://www.ncbi.nlm.nih.gov/pubmed/10625307

Morales La Madrid, A., Hashizume, R., & Kieran, M. W. (2015). Future clinical trials in DIPG: Bringing epigenetics to the clinic. *Frontiers in Oncology, 5*, 148. 10.3389/fonc.2015.00148 Retrieved from http://www.ncbi.nlm.nih.gov/pubmed/26191506

Nguyen, A, Moussalieh, F., Mackay, A., Cicek, E., Coca, A., Chenard, M., Weingertner, N., Lhermitte, B., Letouzé, E., Guérin, E., Pencreach, E., Jannier, S., Guenot, D., Namer, I., Jones, C., and Entz-Werlé, N. "Characterization of the Transcriptional and Metabolic Responses of Pediatric High Grade Gliomas to MTOR-HIF-1α Axis Inhibition." *Oncotarget* 8, no. 42 (2017). doi:10.18632/oncotarget.16500.

Richardson, P. G., Eng, C., Kolesar, J., Hideshima, T., & Anderson, K. C. (2012). Perifosine, an oral, anti-cancer agent and inhibitor of the Akt pathway: Mechanistic actions, pharmacodynamics, pharmacokinetics, and clinical activity. *Expert Opinion on Drug Metabolism & Toxicology, 8*(5), 623-633. doi:10.1517/17425255.2012.681376

Sheehy, R. M., Kuder, C. H., Bachman, Z., & Hohl, R. J. (2015). Calcium and P-glycoprotein independent synergism between schweinfurthins and verapamil. *Cancer Biology & Therapy, 16*(8), 1259-1268. 10.1080/15384047.2015.1056420 Retrieved from http://www.tandfonline.com/doi/abs/10.1080/15384047.2015.1056420

Shoemaker, R. H. (2006). The NCI60 human tumour cell line anticancer drug screen. *Nature Reviews Cancer, 6*(10), 813-823. doi:10.1038/nrc1951

Singh, P., Saxena, R., Srinivas, G., Pande, G., & Chattopadhyay, A. (2013). Cholesterol Biosynthesis and Homeostasis in Regulation of the Cell Cycle. *PLoS ONE, 8*(3). doi:10.1371/journal.pone.0058833

Sorrentino, G., Ruggeri, N., Specchia, V., Cordenonsi, M., Mano, M., Dupont, S., Manfrin, A., Ingallina, E., Sommaggio, R., Piazza, S., Rosato, A., Piccolo, S., and Del Sal, G. "Metabolic Control of YAP and TAZ by the Mevalonate Pathway." *Nature Cell Biology* 16, no. 4 (2014): 357-66. doi:10.1038/ncb2936.

Tallarida, R. J. (2011). Quantitative methods for assessing drug synergism. *Genes & Cancer, 2*(11), 1003. Retrieved from http://www.ncbi.nlm.nih.gov/pubmed/22737266

Vanan, M. I., & Eisenstat, D. D. (2015). DIPG in children - what can we learn from the past? *Frontiers in Oncology, 5*, 237. 10.3389/fonc.2015.00237 Retrieved from http://www.ncbi.nlm.nih.gov/pubmed/26557503

Villa, G., Hulce, J., Zanca, C., Bi, J., Ikegami, S., Cahill, G., Gu, Y., Lum, K., Masui, K., Yang, H., Rong, X., Hong, C., Turner, K., Liu, F., Hon, G., Jenkins, D., Martini, M., Armando, A., Quehenberger, O., Cloughesy, T., Furnari, F., Cavenee, W., Tontonoz, P., Gahman, T., Shiau, A., Cravatt, B., and Mischel, P. "An LXR-Cholesterol Axis Creates a Metabolic Co-Dependency for Brain Cancers." *Cancer Cell* 30, no. 5 (2016): 683-93. doi:10.1016/j.ccell.2016.09.008.

Walsby, E., Lazenby, M., Pepper, C., & Burnett, A. K. (2011). The cyclin-dependent kinase inhibitor SNS-032 has single agent activity in AML cells and is highly synergistic with cytarabine. *Leukemia, 25*(3), 411-419. doi:10.1038/leu.2010.290

Warren, K. E., Killian, K., Suuriniemi, M., Wang, Y., Quezado, M., & Meltzer, P. S. (2012). Genomic aberrations in pediatric diffuse intrinsic pontine gliomas. *Neuro-Oncology, 14*(3), 326-332. 10.1093/neuonc/nor190 Retrieved from http://www.ncbi.nlm.nih.gov/pubmed/22064882

Wenyong Long, Yang Yi, Shen Chen, Qi Cao, Wei Zhao, & Qing Liu. (2017). Potential new therapies for pediatric diffuse intrinsic pontine glioma. *Frontiers in Pharmacology, 8*10.3389/fphar.2017.00495 Retrieved from https://doaj.org/article/d07fc3ad0f2e408e9fde22bec1ddc1f3

Wu, Y. L., Maachani, U. B., Schweitzer, M., Singh, R., Wang, M., Chang, R., & Souweidane, M. M. (2017). Dual Inhibition of PI3K/AKT and MEK/ERK Pathways Induces Synergistic Antitumor Effects in Diffuse Intrinsic Pontine Glioma Cells. *Translational Oncology, 10*(2), 221-228. doi:10.1016/j.tranon.2016.12.008

Zhu, H., Zhang, L., Wu, S., Teraishi, F., Davis, J. J., Jacob, D., & Fang, B. (2004). Induction of S-phase arrest and p21 overexpression by a small molecule 2[[3-(2,3-dichlorophenoxy)propyl] amino]ethanol in correlation with activation of ERK. *Oncogene, 23*(29), 4984-4992. 10.1038/sj.onc.1207645 Retrieved from http://dx.doi.org/10.1038/sj.onc.1207645

Vita

Daniel C. Daugherty

Permanent Address: 6077 Daggett Road, Girard, PA 16417
Current Address: 93A University Manor East, Hershey, PA 17033
daughertyd26@gmail.com (814) 464-4060

OBJECTIVE

Obtain acceptance into a school of medicine.

EDUCATION

Master's of Anatomy *August 2017-2019*
Pennsylvania State University College of Medicine, Hershey, PA
Bachelor of Science in Neuroscience and Biology *May 2017*
Allegheny College, Meadville, PA Overall GPA: 3.26 Science GPA: 3.30

Academic Honors

- *Beta Beta Beta* Biology Honor Society, Allegheny College *2015-2017*
- Alden Scholar (Dean's List), Allegheny College *2014/15, 2015/16, 2016/17*

Organizations

- Allegheny College Pre-Health Club Member *2013-2017*
- Dude's Bible Study *2013-2017*

Relevant Courses:

- Gross Anatomy, Organ Physiology, Neuroanatomy, Histology I, Histology II, Embryology, Organismal Physiology and Ecology, Genetics Development and Evolution, Evolution, Organic Chemistry I, Organic Chemistry II, Biochemistry, Neurophysiology, Neurosensory Biology, Biostatistics, Animal Physiology, Cellular Biology

SKILLS AND ABILITIES

- Animal handling
- Cell culture
- Trained in dissection
- Trained in sterile technique
- Trained in administering intraperitoneal and intramuscular injections to lab animals
- Microsoft Power Point, Microsoft Excel, Microsoft Word

WORK EXPERIENCE

Sales Member, Under Armour, Hershey, PA *Jul 2018-Dec 2018*

- Provide excellent customer service while showing teamwork and working as a cohesive group during retail sales.

Phonathon Supervisor, Allegheny College, Meadville, PA *Oct 2013-2017*

- Call alumni to ask for donations to the college, solidifying alumni relations, and ensure day-to-day performance of other employees.

Scott Enterprises (IHOP/Applebee's), Erie/Meadville, PA *May 2015-Apr 2017*

- Serve guests while helping to prepare food.

TA for Organic Chemistry I, Allegheny College, Meadville, PA *Aug-Dec 2015*

- Provide help for students with lab material and protocol.

Customer Service Associate, Lowe's Home Improvement, Erie, PA

- Operate cash register, provide customer service, and work in other areas if needed.

LEADERSHIP, EXTRACURRICULAR, AND SERVICE EXPERIENCE

Prosection, Penn State Hershey Multidisciplinary Laboratory *May 2018-Jul 2018*

- Dissection of human cadaver to demonstrate anatomic structures for PA students *~20 hours*

Life Church of Hershey, Hershey Pa *May 2018-Present*

- Operate the sound board to follow with church service.

Brave Cubs, Penn State Hershey Children's Hospital *May 2018-Present*

- I am a student handler who escorts people dressed as super heroes or princesses to the pediatric pre-op waiting room. I check with the patient and their family to make sure it is okay for a visitor to enter. We are trying to help children cope with the surgery they face. *~5 hours*

Phonathon Supervisor, Allegheny College, Meadville, PA *Oct 2015-2017*

- Displayed leadership by handling alumni data, credit cards, donations, and supervising other workers.

Health Coach Volunteer, Meadville Medical Center *Jan-Dec 2016*

- Provided health and nutrition guidance to two patients as their Health Coach *~40 hours*

Make a Difference Day, Meadville, PA *Oct 17 2013/2014*

- Provided manual labor to the Meadville community. *12 hours*

SHADOWING AND PROFESSIONAL DEVELOPMENT *2012-Present*

Neuro-oncologist, Dr. Brad Zacharia, Hershey Medical Center/OR, Hershey, PA *14 hours*

- Observed in clinic seeing patients and during an arachnoid cyst surgery.

Pediatric Cardiothoracic Surgeon, Dr. Brain Clark, Hershey Children's Hospital, Hershey PA

- Observed open heart surgery for pulmonary valve replacement. *13 hours*

Otolaryngologist, David Goldenburg, Hershey Medical Center OR, Hershey, PA

- Observed multiple thyroidectomies and a tonsillectomy. *8 hours*

PA/C, Mike Strubel; Neurosurgeon, Brian Dalton, Saint Vincent Hospital OR, Erie, PA

- Learned about spinal fusions as well as brain tumors while closely observing each surgery respectively. Also, visited patients in a clinical setting. *9 hours*

Orthopedic Surgeon, Dr. Stefanovski, UPMC Hamot Offices and OR, Erie, PA

- Observed multiple orthopedic surgeries, including knee and shoulder arthroscopies, and made routine clinical visits**.** *8 hours*

Interventional Cardiologist, Dr. Ward, Saint Vincent Cath Lab, Erie, PA

- Observed multiple heart catheterizations through both radial and femoral arteries. 6 *hours*

Professor of Neuroscience and Psychology, Dr. Connell-Pensky, Meadville, PA

- Learned about the basics of EEG, how to use software to read brain waves, and how to clean equipment. *8 hours*

DaVita Dialysis Center, Meadville, PA *4 hours*

- Exposure to what dialysis is and how it works.

Community Care Network, Meadville, PA *4 hours*

- Experienced multiple home visits to patients of a mobile nurse.

VNA Alliance, Meadville, PA *4 hours*

- Traveled with a Physical Therapist to patient homes to provide therapy.

RESEARCH

Master's Thesis, Penn State University Hershey Cancer Institute *February 2018-April 2019*

Potential Therapies for Diffuse Intrinsic Pontine Glioma Cells

- This experiment is currently testing novel cancer drugs effects on the pediatric brainstem tumor DIPG. In order to simulate current therapies, other potential cancer drugs as well as radiation therapy will be used.

Independent Researcher, Allegheny College Neuroscience Department *Sept 2016-Mar 2017*

The effects of inhaled CO_2 on febrile seizures in the mouse model

- This experiment tested if levels of CO_2 lower than 5% would effectively diminish seizure activity in febrile seizure mice. I found that both 2% and 3% CO_2 both were as effective as 5% CO_2 in controlling seizure activity. Being able to use CO_2 as a treatment for children with febrile seizures as well as all epilepsy patients is much safer than using benzodiazepines, the current treatment.
- Presented:
    - April 2017- Sigma Xi Undergraduate Research Conference, Erie, PA
    - 2nd place in Biology I oral presentations

Research Assistant, Allegheny College Neuroscience Department *Jan-May 2015*
Some Behavioral Effects of Mefloquine: Evaluation of GABAA and GABAB Antagonists in Rats

- The investigation studied the effects of Mefloquine, a primarily prophylactic anti-malarial medication, on behavior. $GABA_A$ and $GABA_B$ antagonists were utilized to localize Mefloquine action and exasperate the behavioral observations seen by administration of Mefloquine alone. The study's ultimate goal was to determine the validity of claims that Mefloquine caused psychotic breaks in patients treated with it prophylactically in the late twentieth century.
- Presented:
    - April 2015- Sigma Xi Undergraduate Research Conference, Erie, PA
    - May 2015- Society for the Quantitative Analyses of Behavior 2015 Conference, San Antonio, TX